NeuroImage 253 (2022) 119125

Contents lists available at ScienceDirect

NeuroImage

journal homepage: www.elsevier.com/locate/neuroimage

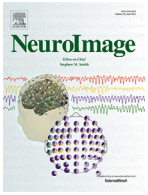

The overlapping modular organization of human brain functional networks across the adult lifespan

Yue Gu[a], Liangfang Li[a], Yining Zhang[a], Junji Ma[a], Chenfan Yang[a], Yu Xiao[a], Ni Shu[b], Cam CAN[c], Ying Lin[a,*], Zhengjia Dai[a,*]

[a] Department of Psychology, Sun Yat-sen University, Guangzhou, China, 510006
[b] State Key Laboratory of Cognitive Neuroscience and Learning & IDG/McGovern Institute for Brain Research, Beijing Normal University, Beijing, China, 100875
[c] Cambridge Centre for Ageing and Neuroscience (Cam-CAN), University of Cambridge and MRC Cognition and Brain Sciences Unit, Cambridge, United Kingdom

ARTICLE INFO

Keywords:
Lifespan
Brain connectome
Overlapping modular organization
Resting-state fMRI

ABSTRACT

Previous studies have demonstrated that the brain functional modular organization, which is a fundamental feature of the human brain, would change along the adult lifespan. However, these studies assumed that each brain region belonged to a single functional module, although there has been convergent evidence supporting the existence of overlap among functional modules in the human brain. To reveal how age affects the overlapping functional modular organization, this study applied an overlapping module detection algorithm that requires no prior knowledge to the resting-state fMRI data of a healthy cohort (N = 570) aged from 18 to 88 years old. A series of measures were derived to delineate the characteristics of the overlapping modular structure and the set of overlapping nodes (brain regions participating in two or more modules) identified from each participant. Age-related regression analyses on these measures found linearly decreasing trends in the overlapping modularity and the modular similarity. The number of overlapping nodes was found increasing with age, but the increment was not even over the brain. In addition, across the adult lifespan and within each age group, the nodal overlapping probability consistently had positive correlations with both functional gradient and flexibility. Further, by correlation and mediation analyses, we showed that the influence of age on memory-related cognitive performance might be explained by the change in the overlapping functional modular organization. Together, our results revealed age-related decreased segregation from the brain functional overlapping modular organization perspective, which could provide new insight into the adult lifespan changes in brain function and the influence of such changes on cognitive performance.

1. Introduction

Lifespan research has become a hot spot with the intensification of global aging (Bookheimer et al., 2019). In neuroscience, mapping how the human brain network (i.e., human connectome) changes across the lifespan can enhance our understanding of neurocognitive development and decline (Zuo et al., 2017). Recent studies usually explore the age-related changes of functional brain network by topological measures of graph theory (Cao et al., 2014; Chandan et al., 2018; Sala-Llonch et al., 2014). Specifically, previous studies on brain functional networks have found the inverted-U trajectories of the local efficiency over the lifespan (Cao et al., 2014), and age-related linearly increase in the shortest-path length and the average clustering coefficient (Sala-Llonch et al., 2014). Additionally, the nodal betweenness was found to decrease in the frontal lobe and occipital lobe while the nodal degree and the nodal efficiency increased in the posterior frontal lobe and parietal lobe over the lifespan (Chandan et al., 2018). These findings implied that age could impact on both functional segregation (i.e., local efficiency and clustering coefficient) and integration (i.e., shortest-path length and nodal betweenness) of the brain network.

Modules, which are derived from a decomposition of the network, are subcomponents that are internally strongly coupled but externally weakly coupled. As an important topological characteristic of the human brain functional network, the functional modular organization has been widely studied (Alexander-Bloch et al., 2010; Bordier et al., 2018; Calhoun et al., 2008; Jones et al., 2012; Liao et al., 2017; Meunier et al., 2009a, 2010). Three essential features of the functional modular organization have been revealed: 1) the identification of modules has shown high reproducibility in each individual (Guo et al., 2012); 2) each module corresponds to specific cognitive performance (Sadaghiani and Kleinschmidt, 2013), such as the visual networks (VIS) supports visual perception (Van Den Heuvel and Pol, 2010)

* Corresponding authors. Department of Psychology, Sun Yat-sen University, Guangzhou, China, 510006.
E-mail addresses: linying23@mail.sysu.edu.cn (Y. Lin), daizhengj@mail.sysu.edu.cn (Z. Dai).

https://doi.org/10.1016/j.neuroimage.2022.119125.
Received 2 December 2021; Received in revised form 2 March 2022; Accepted 19 March 2022
Available online 21 March 2022.

and the fronto-parietal networks (FPN) is involved in initiating and adjusting control (Dosenbach et al., 2008); 3) modularity may promote brain adaptation and increase flexibility in response to a changing environment (Sporns and Betzel, 2016) and prevent catastrophic forgetting (Ellefsen et al., 2015). Modules are subnetworks tightly connected within but loosely connected with others (Sporns and Betzel, 2016). Therefore, neuroscientists often named modules as networks, e.g., visual network, default mode network (Geerligs et al., 2015a; Grady et al., 2016; Moraschi et al., 2020; Power et al., 2011; Rieck et al., 2021; Yeo et al., 2011). In this article, to maintain consistency with previous literature and help readers strictly distinguish the concept of modules and networks, we only referred modules as networks when a prior modular partition was used and the modules were already named as networks in the prior. Recently, several studies have been focusing on the age-related changes in the brain functional modular organization and suggested that brain segregation reduces as age increases (Chan et al., 2014; Meunier et al., 2009a; Spreng et al., 2016). Specifically, lower modularity with weaker intra-module functional connectivity but stronger inter-module functional connectivity was continuously observed across the lifespan (Chan et al., 2014; Geerligs et al., 2015a; Spreng et al., 2016). The age-accompanied functional modular changes were mainly located in the default mode network (DMN), dorsal attention network (DAN), VIS, and FPN (Betzel et al., 2014; Cassady et al., 2020; Ferreira and Busatto, 2013; Grady et al., 2016; Puxeddu et al., 2020; Spreng et al., 2016). Additionally, these age-related changes of the functional modular structure were found associated with cognitive control and attention performance (Betzel et al., 2014).

Currently, the module detection methods used in the above age-related studies mainly focused on non-overlapping modules, that is, each brain region only belongs to a single module. However, neuroimaging studies have suggested that the human brain functional network is more likely to bear an overlapping modular organization (Lin et al., 2018; Najafi et al., 2016; Yeo et al., 2014), in which a brain region can participate in more than one functional module. Previous studies not only provided rich evidence to support the existence of overlap among functional modules (Bassett et al., 2011; Bullmore and Sporns, 2009; Fries, 2005; Power et al., 2013), but also implied that the concept of overlap may pave the way to interpret the flexible and variable relationships between the human brain and cognitive functions in a more realistic manner (Lin et al., 2018; Yeo et al., 2015). In particular, it would be of great interest to study how the overlapping functional modular structure, including the overlapping modules and the overlapping nodes, change across the adult lifespan and how such change induces and/or affects the cognitive functions. However, to date, few studies have examined the changes in overlapping functional modules across the adult lifespan.

To address this issue, we employed resting-state functional magnetic resonance imaging (R-fMRI) to explore the overlapping modular organization of the human brain functional network in 570 healthy participants across the adult lifespan (18–88 years). Firstly, the maximal-clique based multiobjective evolutionary algorithm (MCMOEA; Wen et al., 2016; Lin et al., 2018) was used to identify the overlapping brain functional modular structure of each participant. Secondly, based on the overlapping modules detected, we respectively examined the changing trajectories of the overlapping modules and the overlapping nodes during adult lifespan by regression models and age-based group comparisons. Then, we revealed the functional features of the nodal overlapping probability through functional gradient and flexibility analyses. Finally, we examined how the characteristics of overlapping modules and nodes were related to fluid intelligence and the Benton face recognition test performance, both of which could effectively measure individual memory capacity and were already found sensitive to age (Feng et al., 2020; Kievit et al., 2014).

2. Materials and methods

2.1. Participants

Data of 649 participants [age range 18–88 years; mean = 59.24, standard deviation (SD) = 18.55] were obtained from the second stage of the Cambridge center for Ageing and Neuroscience (Cam-CAN) (http://www.cam-can.org, Shafto et al., 2014). Among these participants, 79 participants were excluded for having one of the following issues: missing data (4 participants), image artifacts (6 participants), and excess head motion (69 participants, details please see "Data acquisition and preprocessing"). Thus, a final sample of 570 participants (age range 18–88 years, mean = 52.88, SD = 18.44, 287 females) was included in our main analyses. All these participants fulfilled the following requests: (1) completed the full MRI testing session and no abnormal anatomical structure was observed, (2) scored at least 25 on the mini mental state examination, (3) had no contraindications to MRI, (4) were native or bilingual English speakers, (5) had normal or corrected-to-normal vision and hearing and (6) no head injury or neurological disorders (Shafto et al., 2014). Ethical approval was obtained from the Cambridge shire Research Ethics Committee and all participants gave their written informed consent prior to participation.

2.2. Data acquisition and preprocessing

The MRI data were collected on a 3T Siemens TIM Trio System, with a 32-channel head coil. Resting-state fMRI (R-fMRI) data were obtained using an echo-planar imaging sequence parameters: repetition time (TR)/echo time (TE) = 1970 ms/30 ms, flip angle = 78°, number of slices = 32, slice thickness = 3.7 mm, voxel size = 3 mm × 3 mm × 4.44 mm, field of view (FOV) =192 mm × 192 mm and total volumes = 261. The 3D T1-weighted structural images were acquired using Magnetization Prepared Rapid Acquisition Gradient-Echo pulse sequences. The sequence parameters were $1 \times 1 \times 1$ mm^3 resolution, TR/TE = 2250 ms/2.99 ms, inversion time (TI) = 900 ms, flip angle = 9°, and FOV = $256 \times 240 \times 192$ mm^3. More details of the data collection can be found in Shafto et al. (2014).

Image preprocessing for R-fMRI was carried out using the Data Processing Assistant for Resting-State fMRI (DPARSF) (http://rfmri.org/DPARSF, Yan and Zang, 2010) toolbox and SPM8 (http://www.fil.ion.ucl.ac.uk/spm). For each participant, the first six volumes were discarded. The realignment was performed after slice timing to the first volume to correct head motion. Sixty-nine participants were excluded for excess head motion (more than 2 mm or 2°). Then, the T1-weighted image was coregistered to the mean functional image after motion correction and then segmented into gray matter, white matter and cerebrospinal fluid tissue images. The head motion corrected functional images were further spatially normalized to the Montreal Neurological Institute (MNI) space using the parameters estimated from T1 unified segmentation (Ashburner and Friston, 2005) and were resampled into 3-mm isotropic voxels. Finally, the normalized functional images were detrended, regressed out the nuisance variables (Friston's 24 head motion parameters, global signal, white matter, and cerebrospinal fluid signals) and temporal band-pass filtered to 0.01–0.08 Hz.

2.3. Construction of brain functional networks

The brain functional network construction was carried out using the graph theoretical network analysis (GRETNA) (http://www.nitrc.org/projects/gretna/, J. Wang et al., 2015). For each participant, we parcellated the whole brain into 264 regions/nodes (Power et al., 2011). Then, we computed the Pearson correlation coefficient between time series of each pair of nodes and generated a 264 by 264 symmetric correlation matrix. Considering the ambiguous biological explanation of negative correlations (Fox et al., 2009;

Murphy et al., 2009), we only preserved positive correlations and set the negative correlations as zeros. A binary and undirected functional network was then constructed by thresholding the matrix with 15% sparsity.

2.4 Detection of overlapping modules

To detect individual overlapping modules in the brain functional network, the maximal-clique-based multiobjective evolutionary algorithm (MCMOEA) (Lin et al., 2018; Wen et al., 2016) was used. Without assuming the number of overlapping modules, this algorithm evolves a population of candidate overlapping modular structures through customized operators to achieve optimal tradeoff between two objectives: maximizing the intra-link density whilst minimizing the linter-link density of modules. The MCMOEA has been found advantageous over a variety of state-of-the-art algorithms in both synthetic and real-world networks (Wen et al., 2016), and it has been successfully applied to detect the overlapping modular structure of healthy young adults (Lin et al., 2018).

The application procedure of MCMOEA used in this study was similar as that introduced by Lin et al. (2018). Firstly, a population of 100 candidate overlapping modular structures were generated. Each of them was linked to a single-objective optimization problem, which was obtained by using the Tchebycheff approach to decompose the original multiobjective optimization problem (Miettinen, 2012). The MCMOEA evolved the population with customized operators until the maximum number of generations reaches 10,000, or the population has not been updated for 500 consecutive generations. The population of the final generation was then returned as the result, which contained 100 nondominated overlapping modular structures with near-optimal tradeoff between intra- and inter-link density. Due to the probabilistic algorithm, the MCMOEA was run for 100 times. Then, we applied the fast nondominated sorting approach (Deb et al., 2002) to find the nondominated solutions among the resulting 10,000 solutions. After removing duplicate solutions, the similarity between two different nondominated solutions was calculated by the generalized normalized mutual information (gNMI; Lancichinetti et al., 2008). The gNMI is an extension of the mutual information in the overlapping context and has been proven reliable (Danon et al., 2005). Higher gNMI scores imply greater similarity between two overlapping modular structures. Therefore, the solution with the maximum average gNMI was supposed to reveal the most typical and robust overlapping modular structure of each participant and was thus selected for subsequent analyses (Lin et al., 2018).

2.5. Analyses of overlapping modules and overlapping nodes

We derived three measures to capture the characteristics of overlapping modules at the individual level: (1) the number of overlapping modules; (2) the overlapping modularity score, which can be used to describe segregation, was proposed by Lázár et al. (2009) for evaluating the properness of an overlapping modular structure based on the contrast between densities of inter- and intra-module connections. Let $C_{i,r}$ denote the connectivity contribution of node i to an overlapping module OM_r, i.e.,

$$C_{i,r} = \frac{\sum_{j \in OM_r,\, i \neq j} a_{i,j} - \sum_{j \notin OM_r} a_{i,j}}{d_i}$$

where $a_{i,j}$ denotes an element in the adjacency matrix of the network, with $a_{i,j} = 1$ for nodes i and j being connected and $a_{i,j} = 0$ for the opposite, d_i denotes the degree of node i. Then the overlapping modularity M^{ov} is calculated

$$M^{ov} = \frac{1}{K} \sum_{r=1}^{K} \left[\frac{\sum_{i \in OM_r} \frac{C_{i,r}}{s_i}}{n_r} \times \frac{n_r^e}{\binom{n_r}{2}} \right]$$

where s_i is the number of overlapping modules node i belongs to, n_r and n_r^e are the numbers of nodes and edges in OM_r, respectively, and K is the number of overlapping modules. (3) the modular similarity, which was calculated as the average gNMI score between the overlapping modular structures of the current participant and of the specified counterparts.

The existence of overlapping nodes (i.e., nodes participating in two or more functional modules) is the signature that distinguishes overlapping modular structure from traditional non-overlapping modular structure, and previous studies have revealed their important roles in promoting network communication and functional flexibility (Lin et al., 2018; Yeo et al., 2014). To capture the characteristics of overlapping nodes, we firstly delineated the spatial pattern of overlapping nodes by visualizing the distribution of the nodal overlapping probability, with the overlapping probability of each node estimated as the percentage of participants in whose modular structure the corresponding brain region participated in two or more modules. Then, four individual-level measures were calculated based on the overlapping nodes: (1) the number of overlapping nodes; (2) the membership diversity of overlapping nodes, which was reflected by the numbers of nodes participating in k modules ($k \geq 2$); (3) the modular overlapping percentage regarding the ten classic non-overlapping functional modules specified by Power et al. (2011) and Cole et al. (2013) (the cerebellum and the unknown modules were excluded to facilitate interpretation) was calculated as

$$MP_a^n = \frac{M_{ON_a}^n}{ON_{\mathrm{a}}}$$

where ON_{a} denotes the total number of overlapping nodes in the functional brain network of participant a, and $M_{ON_a}^n$ is the number of overlapping nodes in n-th classic non-overlapping functional module ($n = 1, 2, \ldots, 10$). (4) the variability in the spatial locations of overlapping nodes with other participants, which was calculated as the average Jaccard distance between the sets of overlapping nodes from the current participant and the specified counterparts.

It should be emphasized that these seven individual measures were not fully independent as they were all derived from the same overlapping modular structure. Yet they focused on different aspects of the overlapping modular structure. In particular, the number of overlapping modules showed the granularity of the brain functional network. The modularity evaluates the properness of an overlapping modular structure based on the contrast between densities of inter- and intra-module connections, and can be used to describe segregation (Cohen and D'Esposito, 2016; Rubinov and Sporns, 2010). Both the overlapping module similarity and overlapping node variability stand for the inter-subject variance, while the former focuses on the overall module structure and the latter lays more emphasis on overlapping node spatial distribution. The membership diversity of overlapping nodes gives detailed information on the extent of overlap between modules. Additionally, the modular overlapping percentage in each of the ten classic non-overlapping modules described the proportion of overlapping nodes in each classic module.

Based on the above measures, we then analyzed the effect of age on the overlapping modular structure in two ways. Firstly, using age as the independent variable, each of the seven individual-level measures as the dependent variable and gender as the covariate, we built both linear and quadratic regression models to test whether age can predict the changes of the modular structure. Note that for the two measures of modular similarity and spatial variability of overlapping nodes, the counterpart herein referred to the entire set of participants. The Bayesian information criterion (BIC) (Schwarz, 1978) was used to determine the optimal regression model for each measure between the linear and quadratic models, and the one-sample t-test was performed on the optimal model for examining the significance of predictors. Secondly, to perform statistical comparisons to evaluate the age-related changes in overlapping modular organization, we divided the participants into three age groups (Young: 18–45 years, 208 participants; Middle: 46–64 years, 169 participants; Old: 65–88 years, 193 participants) to quantify

the between-group differences in the above measures (Backonja et al., 2018; Campbell et al., 2016; Samu et al., 2017). Notably, in the group-based analyses, the context for calculating the nodal overlapping probabilities and the counterparts in the modular similarity and overlapping node spatial variability referred to the participants in the same age group. The significance of the between-group difference was examined by the permutation test (N = 10,000), which randomly shuffled group labels to build null models. The Bonferroni correction [$P < 0.017$ (0.05/3)] was used to counteract the potential bias induced by multiple comparisons across the three age groups.

To further explore whether and how the functional roles of overlapping nodes were influenced by age, we computed the Pearson correlation coefficients between the nodal overlapping probabilities and two functional indicators across the adult lifespan and the three age groups. The two functional indicators were the nodal gradient and functional flexibility. In particular, the voxel-wise gradient map was built based on gradient 1 that depicted a principal gradient of cortical organization in the human connectome (Margulies et al., 2016). The principal gradient was accounted for the greatest variance in functional connectivity in the brain, and tracked a functional hierarchy from primary sensory processing to higher-order functions such as social cognition (Margulies et al., 2016). A high gradient value implies a larger contribution to higher-order functions. The voxel-wise functional flexibility values were derived by Yeo et al. (2015) from 10,449 cognitive experiments, with a larger value indicating a high probability of being activated by multiple cognitive components. The functional indicators for each of the 264 nodes were then calculated by averaging the voxel-wise indicator values over all the voxels within the corresponding region.

Finally, to assess whether and how the brain functional modular organization was related to the cognitive performance during the adult lifespan, we computed the Pearson correlation coefficients between cognitive performance and each of the above individual-level measures regarding overlapping modules/overlapping nodes. There has been a general agreement that memory performance declines with age (Craik, 1994). We thus chose two memory-related tasks (i.e., fluid intelligence and Benton face recognition test), on which performance has shown age-related decreases in previous Cam-CAN studies (Feng et al., 2020; Kievit et al., 2014). Fluid intelligence is the core of psychometric analyses of intelligence, which has been defined as the ability to think logically and solve problems in the absence of task-specific knowledge and has been found related to working memory (Carpenter et al., 1990). Here, the fluid intelligence was calculated by the sum of Cattell test score on four subtests (Cattell, 1971). The summary score of the Benton face recognition test is a commonly used neuropsychological instrument that tested individual's baseline visual perception and memory (Benton et al., 1994). Higher scores of fluid intelligence and the Benton face recognition test imply better cognitive abilities, especially memory performance. Note that the correlation analyses were only performed on the participants with the corresponding task data (fluid intelligence: N = 553; Benton face recognition test: N = 550). To further explore whether the individual-level overlapping module or node characteristics mediated the age effects on cognitive performance, a mediation analysis was performed using the PROCESS plugin in SPSS (Hayes, 2017; Preacher and Hayes, 2004, 2008). Then, the bootstrap (n = 5000) was performed to assess the statistical significance of the mediation analysis, for which a 95% confidence interval (CI) without zero was equivalent to a significance level of 0.05 (Preacher and Hayes, 2004, 2008).

2.6. Validation analyses

To evaluate the reproducibility of our results, we examined the influences of head motion, global signal, and network sparsity. Firstly, although our main analyses have moderated the influence of head motion by filtering participants and regressing related parameters (Friston et al., 1996) in preprocessing (Yan et al., 2013), we found the mean frame-wise displacement (mFD; Jenkinson et al., 2002) positively correlated with age in our data (R = 0.44, $P < 10^{-3}$). Therefore, we added mFD as an additional covariate in all age-related regression analyses for validation. Secondly, since previous studies have found that global signal regression can introduce negative correlations and reshape the distribution of functional connectivity across the whole brain (Fox et al., 2009; Murphy et al., 2009), we re-performed the main analyses on the data without regressing out global signals. Finally, the network sparsity has been found an influential factor on the results of mainstream module detection algorithms, including MCMOEA (Wen et al., 2016). For validation, we repeated the main analyses over the sparsity of 10% and 20%.

3. Results

3.1. Adult lifespan changes of overlapping modules

Among the three measures for characterizing the overlapping modules, a significant influence of age was found on the overlapping modularity (Fig. 1A-B) and the modular similarity (Fig. 1C-D), but not on the number of overlapping modules. In detail, the overlapping modularity showed negative correlation with age (R = −0.204, $P < 10^{-3}$; Fig. 1A). The overlapping modularity within the elderly group was significantly lower than that of the other two age groups (Old < Young: P = 0.002; Old < Middle: $P < 10^{-3}$; Fig. 1B). These results implied that the functional segregation capability of the human brain gently decreased across the adult lifespan. The modular structure similarity calculated in the context of the entire population was found negatively correlated with age (R = −0.417, $P < 10^{-3}$; Fig. 1C). In addition, the modular structure similarity calculated within each age group coincided with the above decreasing trend, and the permutation test confirmed that the differences of the modular structure similarity between age groups were all significant (Young > Middle > Old: all $P < 10^{-3}$; Fig. 1D). These results suggested that the overlapping modular structure of the human brain functional network was getting more individual variability as age increased.

3.2. Adult lifespan changes of overlapping nodes

The distribution of nodal overlapping probabilities calculated from the entire population of participants and each of the three age groups (Fig. S1). Overall, the nodal overlapping probability calculated from the whole population was higher in the superior frontal gyrus, inferior frontal gyrus, inferior parietal gyrus, and insula, but lower mainly in the postcentral gyrus, parahippocampal gyrus, lingual gyrus, cuneus gyrus, and occipital lobe (Fig. S1A). Similar distribution patterns were also observed in the three age groups (Fig. S1B-D).

The number of overlapping nodes linearly increased along adult lifespan (R = 0.149, $P < 10^{-3}$, Fig. 2A), particularly for overlapping nodes that participated in two and three overlapping modules (k = 2: R = 0.142, P = 0.001; k = 3: R = 0.131, P = 0.004; Fig. 2B), but not for the overlapping nodes participating in four or more modules ($k \geq 4$). Between-group comparisons further confirmed that the old group had significantly more overlapping nodes (Old > Young and Old > Middle: all $P < 10^{-3}$; Fig. 2C) and significantly higher membership diversity (k = 2 or 3) (Old > Young and Old > Middle: all $P \leq 0.006$; Fig. 2D) than each of the other two age groups. Additionally, although the overlapping nodes were found distributed in all the ten classic non-overlapping modules, DMN had the largest modular overlapping percentage considered either across the entire adult lifespan or within each age group (Fig. 3A-B). We found that the modular overlapping percentage linearly increased with age in VIS (R = 0.148, P = 0.002), but linearly decreased in FPN (R = −0.129, P = 0.008; Fig. 3C). Between-group comparison analyses also showed that compared with the old group, the modular overlapping percentage of the young group was significantly lower in VIS ($P < 10^{-3}$) but remained higher in FPN with a marginally significant difference (P = 0.020, Bonferroni-corrected, Fig. 3D).

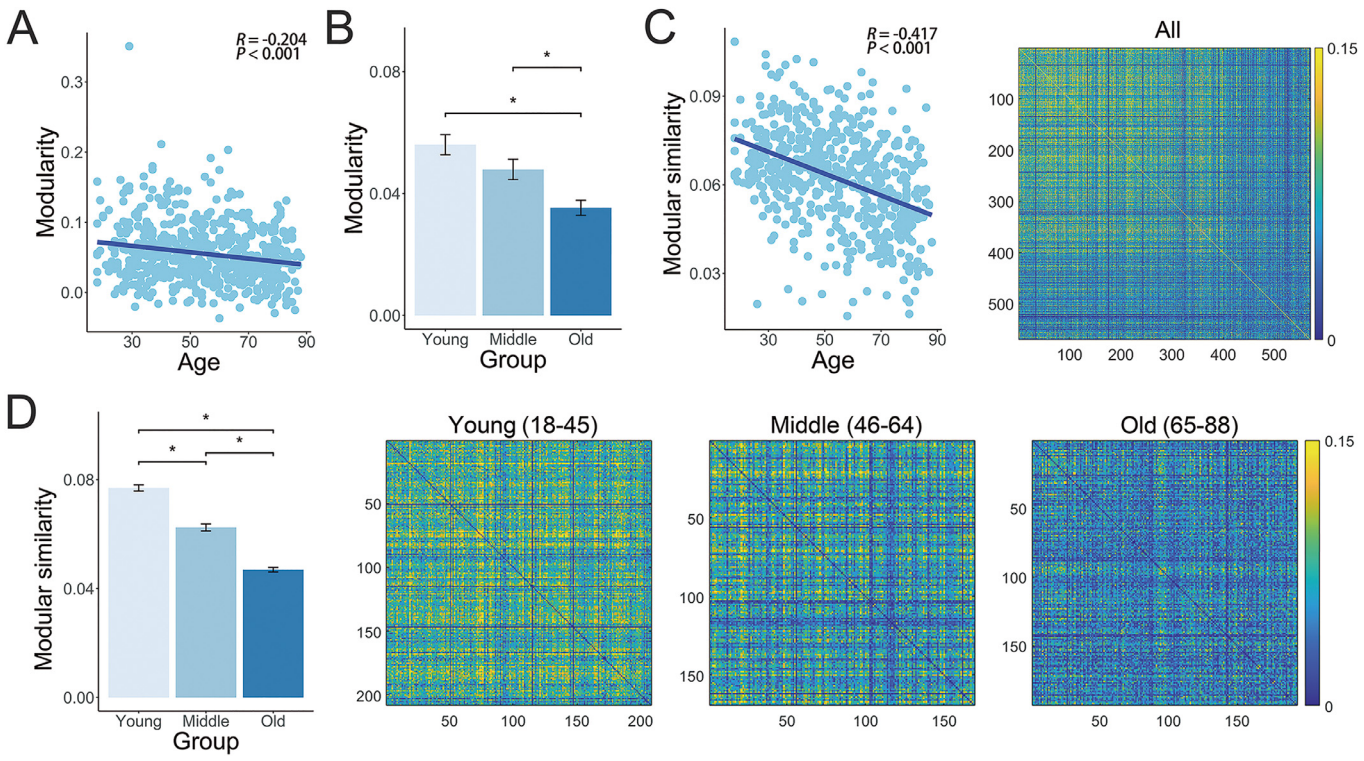

Fig. 1. Lifespan changes in overlapping modules regarding (A & B) modularity and its between-group comparison, (C & D) modular similarity and its between-group comparison. In bar plot, the asterisk indicates significant between-group difference ($P < 0.05$, 10,000 permutations, Bonferroni-corrected).

Further, Fig. 4 showed the regions whose overlapping probabilities exhibited significant between-group differences, including 1) left superior frontal gyrus between the young and middle groups (Middle > Young, $P < 10^{-3}$), 2) left thalamus and left superior parietal lobule between the young and old groups (Old > Young, $P < 10^{-3}$), 3) left superior frontal gyrus (Old < Middle, $P < 10^{-3}$) and left thalamus between the middle and old groups (Old > Middle, $P < 10^{-3}$). Moreover, the individual variability in the spatial pattern of overlapping nodes decreased as age increased ($R = -0.119$, $P = 0.005$; Fig. 5A), and significant differences were detected between the old group and each of the other two groups (Old < Young: $P < 10^{-3}$, Old < Middle: $P = 0.002$; Fig. 5B).

3.3. Adult lifespan changes in the functional characteristics of overlapping nodes

The nodal overlapping probability was found positively correlated with the gradient 1 map of Margulies et al. (2016) ($R = 0.397$, $P < 10^{-3}$; Fig. 6A), and this positive correlation maintained within each age group (Young, $R = 0.362$, $P < 10^{-3}$; Middle, $R = 0.416$, $P < 10^{-3}$; Old: $R = 0.339$, $P < 10^{-3}$; Fig. 6B). In addition, the nodal overlapping probability was also found positively correlated with the functional flexibility map of Yeo et al. (2015) ($R = 0.401$, $P < 10^{-3}$; Fig. 6C). The positive correlations also maintained within each group (Young, $R = 0.397$, $P < 10^{-3}$; Middle, $R = 0.324$, $P < 10^{-3}$; Old, $R = 0.394$, $P < 10^{-3}$; Fig. 6D). These results revealed that the overlapping nodes tended to have higher functional gradient and flexibility.

3.4. Relationships between characteristics of overlapping modules or nodes and cognitive performances

Significant age-related decrease was found in fluid intelligence and Benton face recognition test score ($R = -0.448$, $P < 10^{-3}$; $R = -0.669$, $P < 10^{-3}$). Also, significant difference was found in these two indicators between each pair of age groups by using the permutation test (all $P < 0.05$). For fluid intelligence, we found that it had positive correlations with the overlapping modularity ($R = 0.167$, $P < 10^{-3}$), the modular similarity ($R = 0.367$, $P < 10^{-3}$, Fig. 7A). In contrast, we found that fluid intelligence had negative correlations with the number of overlapping nodes ($R = -0.134$, $P = 0.002$), the number of overlapping nodes that participated in three overlapping modules ($k = 3$: $R = -0.138$, $P = 0.001$), and the modular overlapping percentage in VIS ($R = -0.156$, $P < 10^{-3}$, Fig. 7B). As for the Benton face recognition test score, similar as the patterns of fluid intelligence, it was found positively correlated with the overlapping modularity ($R = 0.149$, $P < 10^{-3}$) and the modular similarity ($R = 0.252$, $P < 10^{-3}$, Fig. 7C), but negatively correlated with the modular overlapping percentage in VIS ($R = -0.148$, $P < 10^{-3}$, Fig. 7D). Above results were all false discovery rate (FDR) corrected.

Additionally, we found that the decrease in the overlapping modular similarity was associated with age (path a: $\beta = -0.436$, $P < 10^{-3}$). After controlling the influence of age, the higher overlapping modular similarity was related to higher fluid intelligence (path b: $\beta = 0.092$, $P < 10^{-3}$). After considering the effect of overlapping modular similarity, the effect of age on fluid intelligence was weakened (path c': $\beta = -0.629$, $P < 10^{-3}$, from path c: $\beta = -0.669$, $P < 10^{-3}$, Fig. 8A). This mediation analysis revealed that overlapping modular similarity was a significant mediator (indirect effect = −0.040, 95% CI = [−0.068, −0.013]) and could partially explain the negative association between age and fluid intelligence (Fig. 8A). Besides, we found that the increase of the modular overlapping percentage in VIS was associated with age (path a: $\beta = 0.149$, $P < 10^{-3}$). After controlling the influence of age, the higher modular overlapping percentage in VIS was related to the lower Benton face recognition test score (path b: $\beta = -0.077$, $P < 10^{-3}$). After considering the effect of modular overlapping percentage in VIS, the effect of age on Benton face recognition test score was weakened (path c': $\beta = -0.473$, $P < 10^{-3}$, from path c: $\beta = -0.484$, $P < 10^{-3}$, Fig. 8B). This mediation analysis revealed that modular overlapping percentage in VIS

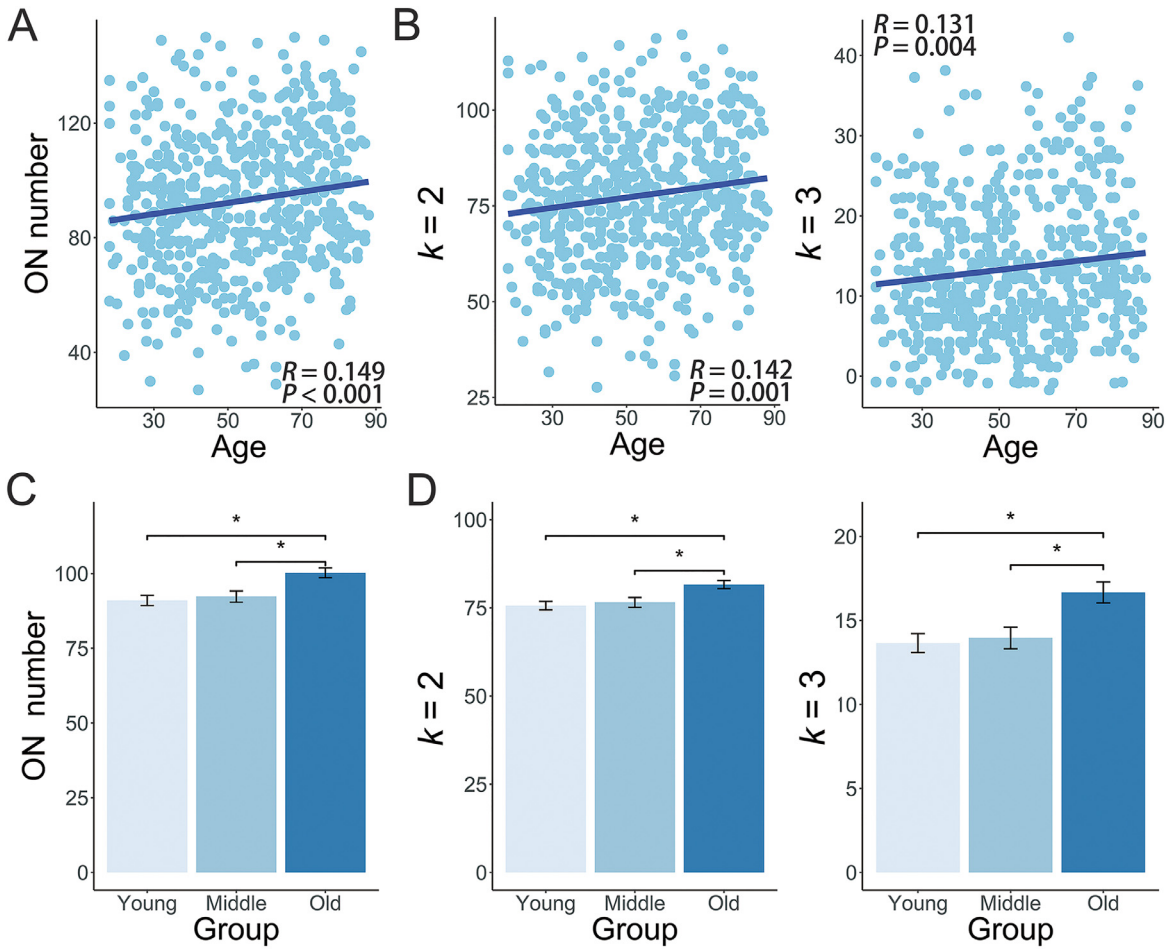

Fig. 2. Lifespan changes in overlapping nodes (ON) regarding (A) number, (B) the membership diversity, the between-group comparison of (C) number and (D) the membership diversity. The light blue nodes denote participants, and dark blue lines denote the aging regression line for linear model. In bar plot, the asterisk indicates significant between-group difference ($P < 0.05$, 10,000 permutations, Bonferroni-corrected).

was a significant mediator (indirect effect = −0.011, 95% CI = [−0.026, −0.001]) and could partially explain the negative association between age and Benton face recognition (Fig. 8B).

3.4. Validation results

We evaluated the influence of head motion, global signal, and network sparsity on our main results. The main results remained largely unchanged in the former two conditions. As for global signal removal, most results coincided with our main findings, but some characteristics (e.g., number of overlapping nodes) were no longer significantly correlated with age, which suggested that the adult lifespan changes might be buried into systematic and physiological noise. For more details, refer to the supplementary materials (Fig. S2 to Fig. S16).

4. Discussion

In this study, we studied the change of the overlapping functional modular organization across the adult lifespan. In terms of overlapping functional modules, the overlapping modularity and the modular similarity both gradually declined linearly over the adult lifespan. In terms of the overlapping nodes, the number increased linearly with age. As for their distribution, the modular overlapping percentage linearly increased in VIS but decreased in FPN with age. Besides, the individual variability in the spatial distribution of overlapping nodes linearly decreased over the adult lifespan. Both the nodal functional gradient and flexibility were positively correlated with the nodal overlapping probability during the adult lifespan and in each age group. Finally, the age-related characteristics of overlapping modules and overlapping nodes were found correlated with memory-related cognitive performance. Together, our results indicated lifespan decreased segregation of the brain functional modular organization, providing new insight into the age-related changes in brain function and behavioral performance.

4.1. Adult lifespan changes of overlapping modules

Modularity, which measures how well a network can be decomposed into a set of sparsely inter-connected but densely intra-connected modules (Newman, 2004), is an advanced topological property of brain network organization and can be used to evaluate functional segregation (Meunier et al., 2009b). The present study found that the overlapping modularity of the brain functional network linearly decreased over the adult lifespan, which is consistent with the findings in non-overlapping modularity studies (Betzel et al., 2014; Cao et al., 2014; Geerligs et al., 2015a). These consistent findings of declined modularity in the elderly revealed that aged brains had decreased intra-module functional connectivity and increased inter-module functional connectivity, which suggests the brain functional network of older people to be less segregated or less differentiated (Betzel et al., 2014; Chan et al., 2014; Geerligs et al., 2015a). The dedifferentiation theory suggests that overactivation of brain regions in the elderly during cognitive tasks may be caused by the decrease in functional distinction between regions (Baltes and Lindenberger, 1997; Park et al., 2004), which may further

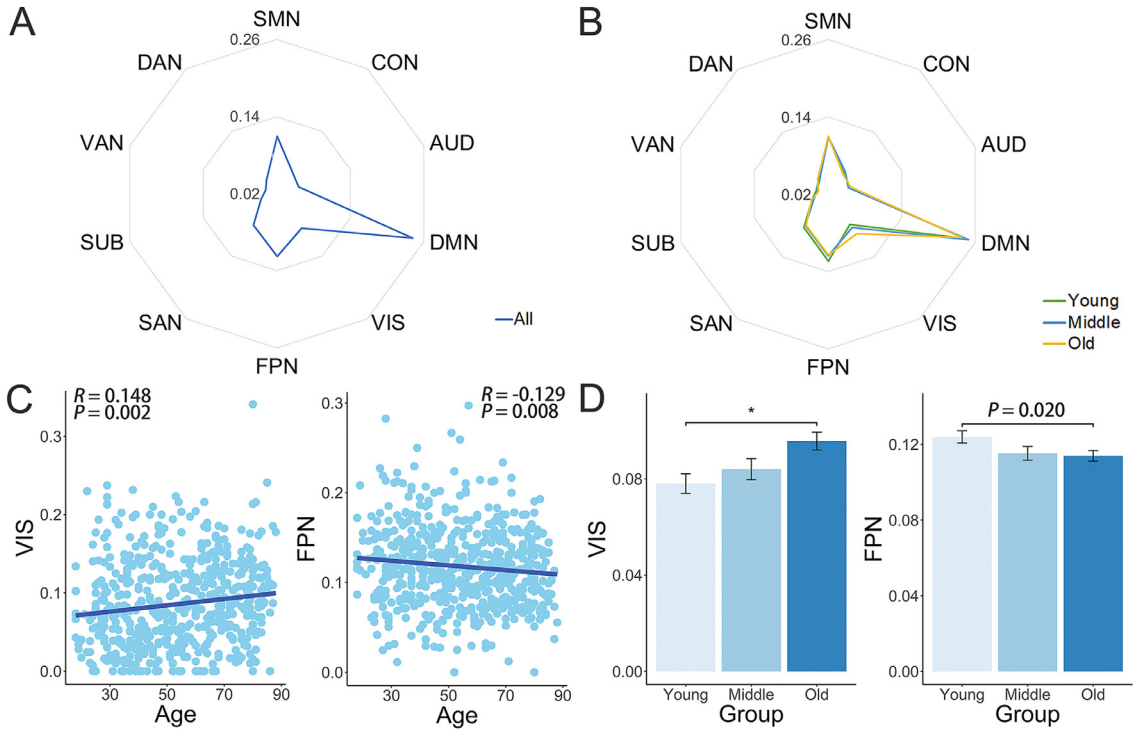

Fig. 3. Lifespan changes in overlapping nodes (ON) regarding (A & B) the distribution in ten classic non-overlapping modules, (C) the modular overlapping node percentage and (D) its between-group comparison. The light blue nodes denote participants, and dark blue lines denote the aging regression line for linear model. In bar plot, the asterisk indicates significant between-group difference ($P < 0.05$, 10,000 permutations, Bonferroni-corrected). Abbreviations: FPN, fronto-parietal network; CON, cingulo-opercular network; SAN, salient network; DAN, dorsal attention network; VAN, ventral attention network; DMN, default mode network; SMN, somatosensory-motor network; AUD, audial network; VIS, visual network; SUB, subcortical network.

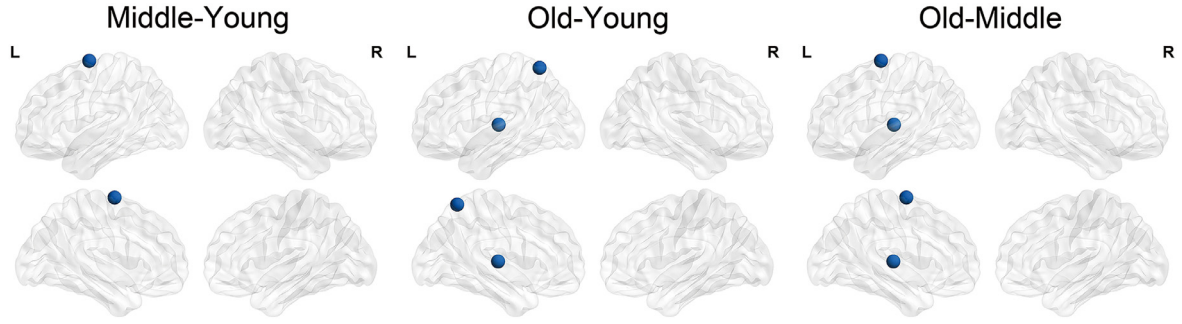

Fig. 4. Between-group differences of the nodal overlapping ratio. The dark blue node indicates significant between-group difference ($P < 0.001$, 10,000 permutation).

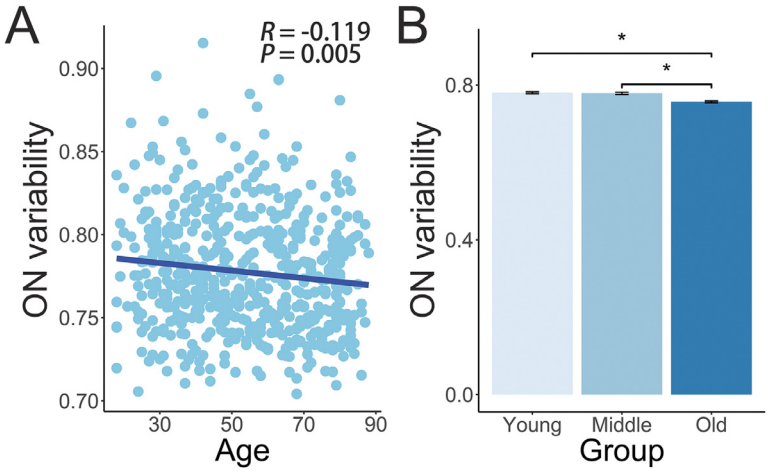

Fig. 5. Lifespan changes in overlapping nodes (ON) regarding (A & B) similarity of spatial distribution. The light blue nodes denote participants, and dark blue lines denote the aging regression line for linear model. In bar plot, the asterisk indicates significant between-group difference ($P < 0.05$, 10,000 permutations, Bonferroni-corrected).

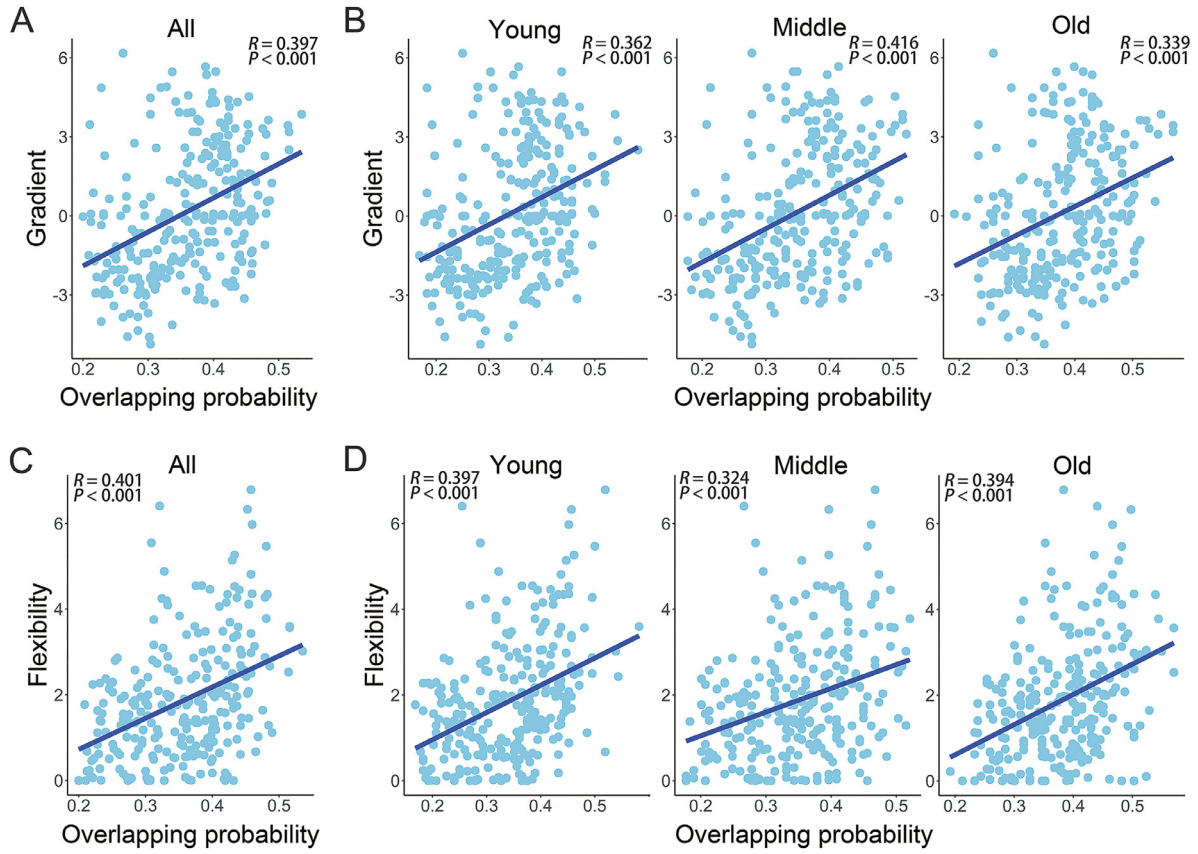

Fig. 6. Lifespan changes in the functional characteristics of overlapping nodes (ON) overlapping probability functional characteristics regarding (A & B) gradient 1, (C & D) functional flexibility. The light blue nodes denote participants, and dark blue lines denote the aging regression line for linear model.

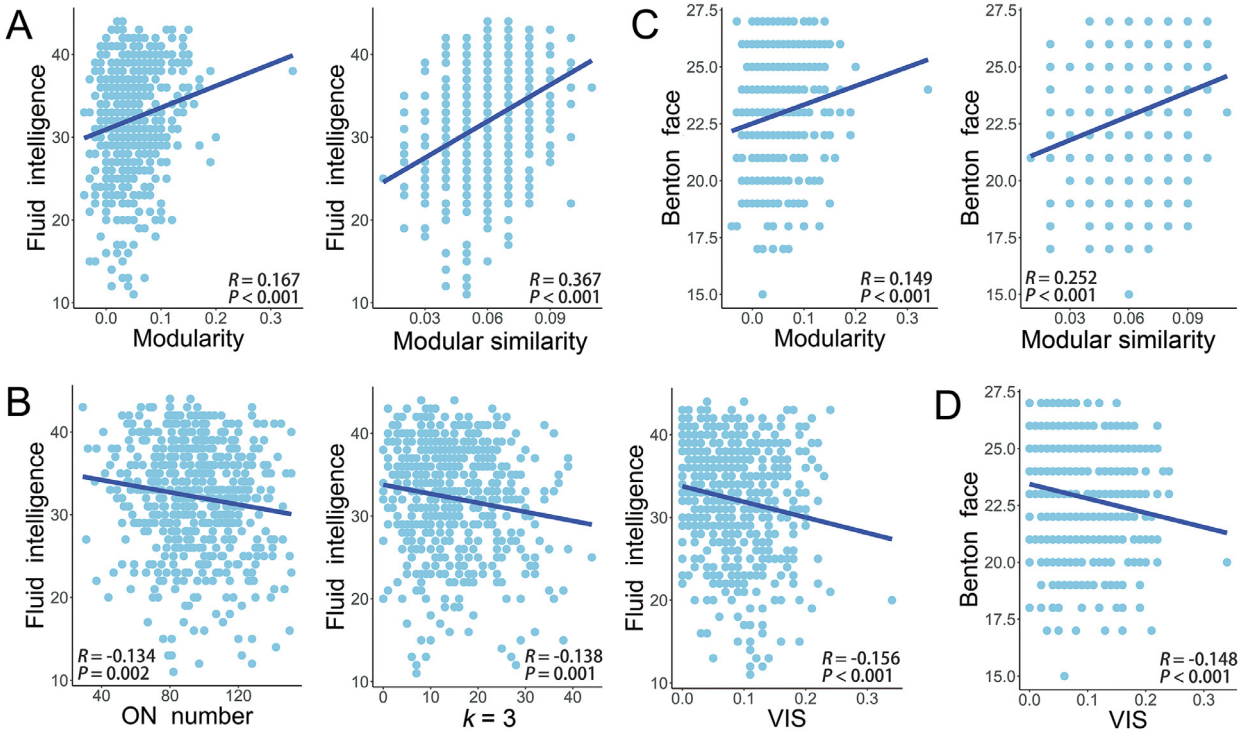

Fig. 7. Relationship between characteristics of overlapping modules (OM) or nodes (ON) and cognitive performances including (A & B) fluid intelligence and (C & D) Benton face recognition test. The light blue nodes denote participants, and dark blue lines denote the aging regression line for linear model ($P < 0.05$, FDR-corrected).

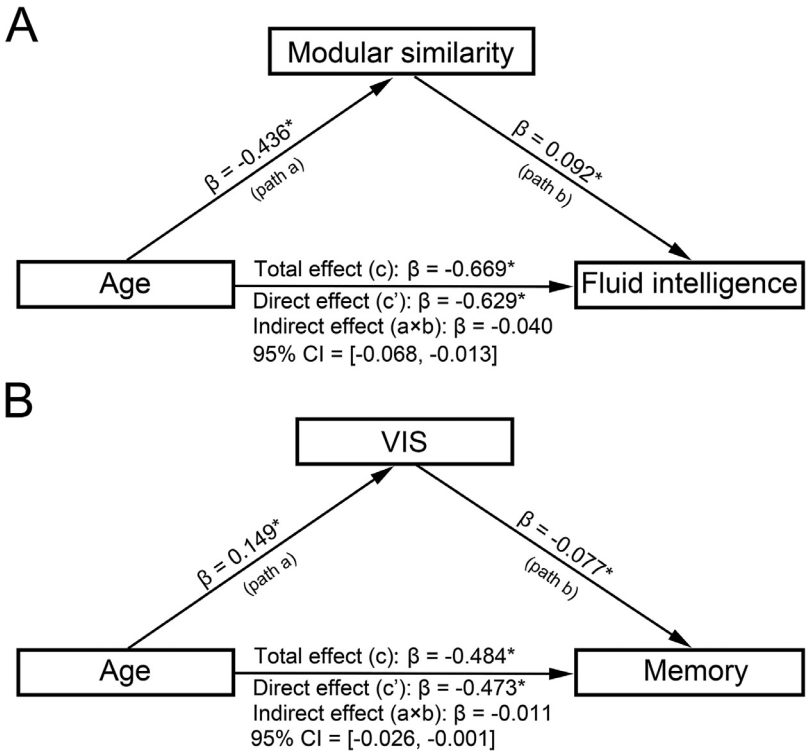

Fig. 8. Mediating effects of overlapping module or node characteristics on lifespan changes in (A) fluid intelligence and (B) memory stands for Benton face recognition test performance. Standardized regression coefficients were reported, and the asterisk indicates significant relationship.

induce the functional module-level dedifferentiation, as observed in the current study. Additionally, previous studies have suggested that there were associations between functional connectivity and structural connectivity across the lifespan (Betzel et al., 2014; Zimmermann et al., 2016; for review, see Damoiseaux, 2017). Betzel et al. (2014) found that the decline in the number of structural connectivity and the network segregation (i.e., non-overlapping modularity) of functional brain network in the elderly. Meanwhile, the relationship between functional connectivity and age depended on the length of shortest paths of structural connectivity. We thus speculated that our finding on the age-related decline in overlapping modularity might also be associated with the age-related changes in the number and the path length of structural connectivity. Our findings provided direct support for the dedifferentiation phenomenon at the functional module level, which could also account for the less distinctive neural representations in old age (Li et al., 2001).

The overlapping modular similarity showed a significant decrease during the adult lifespan. This decreasing trend was also confirmed among age groups. It is consistent with previous studies, which found that the shape and size of modules in elderly are more variable than those of young adults (Chen et al., 2021). Previous studies have also demonstrated that the inter-individual functional connectivity variability increased in the elderly (Garzón et al., 2021; Geerligs et al., 2015b; Ma et al., 2021). Moreover, Song et al. (2014) found that the older group had a higher inter-individual variability in modularity and local efficiency. Wink (2019) found that the eigenvector centrality variation was less consistent in some modules (e.g., medial visual, executive control and left frontoparietal networks) among older adults. These findings were all supportive of the increased inter-individual functional connectivity variability in the older group, as our finding regarding the age-related decrease in overlapping modular similarity. Additionally, Garzón et al. (2021) has suggested that age-related connectome dissimilarity may be attributed to changes in gray matter density. Our results on decrease in overlapping modular similarity were consistent with those of Garzon et al.'s, and thus might also imply similar change in the brain structure. The individual overlapping modular structure variability can further give rise to the growing individual difference in external cognitive/behavioral capability (e.g., fluid intelligence, motor performance, memory) over the lifespan (Carr et al., 2017; Grady, 2012; Ma et al., 2021).

4.2. Adult lifespan changes of overlapping nodes

During the adult lifespan, regions in the superior frontal gyrus, inferior frontal gyrus, inferior parietal lobe and angular gyrus were found to have high overlapping probabilities, suggesting that these regions may play important roles in inter-module interaction. It is worth noting that these regions are mainly located in modules serving as the neural substrate of high-order cognitive functions. In particular, the superior frontal gyrus, inferior frontal gyrus and angular gyrus belong to DMN, and the inferior parietal lobe belongs to FPN. The potential roles of the DMN include working memory (Greicius et al., 2003) and the interplay between emotional processing and cognitive functions (Gusnard et al., 2001; Raichle et al., 2001). The FPN is associated with a wide variety of tasks by initiating and modulating cognitive control abilities (Dosenbach et al., 2008). Moreover, among the ten classic non-overlapping modules (Cole et al., 2013; Power et al., 2011), the overlapping nodes detected over the entire adult lifespan and in all age groups were mainly concentrated in DMN. Additionally, we found that the regions with low nodal overlapping probabilities (e.g., the postcentral gyrus, parahippocampal gyrus and lingual gyrus) were mostly involved in primary functional modules. Thus, these results suggest that higher-order associative modules are more likely to embed overlapping nodes, which was largely compatible with previous overlapping module studies in healthy young adults (Lin et al., 2018; Yeo et al., 2014). Notably, a similar nodal overlapping probabilities distribution existed over the adult lifespan, suggesting relative preservation of the crucial roles of these regions.

Besides the distribution of overlapping nodes, we also examined how the characteristics of overlapping nodes changed during the adult lifespan. We found a significant linear increase of the overlapping node number during the adult lifespan. Moreover, the old group had a significantly larger overlapping node number than the other two groups did. The

increased overlapping node numbers in the elderly implied that more brain regions were involved in multiple modules, which may result in decreased modularity and less differentiation. The age-related increase of the overlapping node membership diversity also supports this conjecture. Further, we found that the modular overlapping percentage in VIS linearly increased with age, which is probably related to previous findings that VIS has an age-related increase in inter-module functional connectivity (Geerligs et al., 2015a; Malagurski et al., 2020) and gradient values (Bethlehem et al., 2020), suggesting that the role of VIS in inter-network information communication becomes more important as age increases. On the other hand, the modular overlapping percentage of FPN linearly decreased during the adult lifespan. The FPN, involved in initiating and modulating control (Dosenbach et al., 2008), was one of the first modules to deteriorate as a result of aging (Nyberg et al., 2010; Raz et al., 1997). With the age-related increase in the total number of overlapping nodes in each individual, the modular overlapping percentage of FPN decreased relatively at the same time. Therefore, our results might provide a potential explanation for the impairment of cognitive control abilities in older people.

Additionally, the overlapping probability of the region in the left thalamus was higher in the older group than in the other groups, indicating that this region was more likely to participate in multiple functional modules in older people. The thalamus is involved in multiple cognitive functions, which is an integrative hub for functional brain networks (Hwang et al., 2017). Previous studies have found that older adults exhibited stronger functional connectivity between the thalamus and putamen, which highlights the potential role of enhanced thalamic connectivity in protecting the memory ability from aging (Ystad et al., 2010). Also, the region in the left superior parietal lobule had higher overlapping probabilities in the old group than in the young group, which was also associated with working memory (Jager et al., 2006). Thus, we speculated that regions with higher overlapping probabilities in the elderly might be the compensation for the age-related decrease in functional connectivity.

The results on the functional characteristics showed that the regions with higher nodal overlapping probability tended to have higher gradient value and higher flexibility during the adult lifespan. This positive relationship was also confirmed in each age group. Previous studies have suggested that the regions with high gradience had the greater variance in functional connectivity (Margulies et al., 2016), and may contribute more to the implementation of higher-order functions (Huntenburg et al., 2018). Moreover, the regions with higher flexibility are associated with a larger variety of cognitive components and may participate in more cognitive tasks (Lin et al., 2018; Yeo et al., 2015). The above findings are thus another evidence for the important functional role of overlapping nodes across development and aging, in particular for their effect in promoting brain system interplay (Lin et al., 2018). It also implies the importance of analyzing overlapping structures for understanding brain functional changes during the adult lifespan and across age groups.

In general, we found that the indicators capturing decreased characteristics of overlapping modules and overlapping nodes during the adult lifespan (e.g., overlapping modular similarity) tended to have positive correlations with fluid intelligence and the Benton face recognition scores. Conversely, the indicators capturing increased characteristics of overlapping modules and overlapping nodes during the adult lifespan tended to have negative correlations. Combining these results with previous findings that fluid intelligence and the Benton face recognition test score was positively related to memory performance (Benton et al., 1994; Cattell, 1971) and declined with age (Feng et al., 2020; Kievit et al., 2014), we speculated that the age-related changes in overlapping modules and overlapping nodes were closely associated with the age-accompanied decline in memory ability. For some weak correlations, they need to be interpreted with caution and require further validation in future studies. In addition, we found that the overlapping modular similarity and the overlapping percentage of VIS partially mediated the negative associations of age with fluid intelligence and the Benton face recognition test score, respectively. Besides, the mediation effect of overlapping modular similarity on lifespan changes in fluid intelligence was maintained in most validation results. Thus, the overlapping modular similarity might serve as a biomarker for aging. Together, these results further supported our conjecture that the age-related changes in the overlapping functional modular organization were possible neural representations of cognitive performance change across the lifespan.

4.3. Future consideration

Several methodological limitations need further considerations. First, the functional atlas used in our study was obtained by exploring a combination of meta-analysis of functional connectivity in an adult population (Power et al., 2011). Ideally, individual functional atlas should be determined by each participant-specific functional connectivity for individual analysis. Several studies have focused on the methodology of individualized functional atlas (Cui et al., 2020; Kong et al., 2019; D. Wang et al., 2015). However, there is still not yet a uniformly recognized golden method about the individualized functional atlas. Future improvement in atlas-related methodological research may help us to further validate and deepen our findings based on reliable individualized functional atlas. Second, the current overlapping method MCMOEA is only feasible for binary networks, because the concept of its first step, the maximum cliques, do not applicable to weighted networks. Nevertheless, the weights do carry additional information about the functional connectivity and may help to gain further insights into overlapping modules. Thus, a future direction is to extend and adapt MCMOEA to weighted networks. Third, whether the global signals should be removed is currently still debatable in the preprocessing procedure of the R-fMRI data. Both our study and previous ones have found relatively large differences between results with and without regressing out the global signals (Li et al., 2016; Murphy et al., 2009; Yang et al., 2014). Future studies are necessary to propose better approaches to minimize the noise in R-fMRI and to evaluate the optimal approaches to analyze the global signals. Fourth, negative correlations were disregarded in our study as the physiological interpretations of negative correlations in resting-state functional MRI remain ambiguous (Murphy et al., 2009; Murphy and Fox, 2017; Fox et al., 2009; Telesford et al., 2011). This method is widely used in functional brain network studies (Lin et al., 2018; Sporns and Betzel, 2016; Wen et al., 2019; Zhang et al., 2021). Computational methods and theories regarding topological analyses in negative correlations and signed functional networks still need to be further developed. Fifth, previous findings showed that the age-related perfusion changes in the human brain (Grunewald et al., 2021; Salami et al., 2016; Staffaroni et al., 2019), and the perfusion level was also associated with functional connectivity (Liang et al., 2013; Zhang et al., 2022). Thus, the age-related change in perfusion may also influence our results. Future studies should further validate our findings after eliminating the perfusion influence in fMRI data. Last, although the current research dataset already covers a wide age range, it is still not a longitudinal/follow-up dataset that covers the whole adult lifespan of each participant. In the future, further validation based on true follow-up data should be considered.

Credit authorship contribution statement

Yue Gu: Methodology, Formal analysis, Writing – review & editing. **Liangfang Li:** Formal analysis, Writing – review & editing. **Yining Zhang:** Formal analysis, Methodology. **Junji Ma:** Formal analysis. **Chenfan Yang:** Methodology. **Yu Xiao:** Methodology. **Ni Shu:** Writing – review & editing. **Ying Lin:** Conceptualization, Methodology, Supervision, Writing – review & editing. **Zhengjia Dai:** Conceptualization, Methodology, Supervision, Writing – review & editing.

Acknowledgment

This work was supported by the National Natural Science Foundation of China (NSFC) (no. 61772569), Guangdong Basic and Applied Basic Research Foundation (no. 2019A1515012148, 2021A1515010844), the Fundamental Research Funds for the Central Universities (no. 19wkzd20, 20wkzd11), and the Open Research Fund of the State Key Laboratory of Cognitive Neuroscience and Learning (no. CNLYB2001).

Ethics statement

Data of the current study were obtained from a public dataset Cambridge center for Ageing and Neuroscience (Cam-CAN). The Cam-CAN was approved by the University of Cambridge, launched in October 2010. All participants had provided written informed content.

Data and Code Availability Statement

The Cam-CAN data is publicly available in the database of Cambridge center for Ageing and Neuroscience: https://www.cam-can.org/. All the toolboxes and third-party codes we used are all stated and cited appropriately.

Supplementary materials

Supplementary material associated with this article can be found, in the online version, at doi:10.1016/j.neuroimage.2022.119125.

References

Alexander-Bloch, A.F., Gogtay, N., Meunier, D., Birn, R., Clasen, L., Lalonde, F., Lenroot, R., Giedd, J., Bullmore, E.T., 2010. Disrupted modularity and local connectivity of brain functional networks in childhood-onset schizophrenia. Front. Syst. Neurosci. 4, 147. doi:10.3389/fnsys.2010.00147.

Ashburner, J., Friston, K.J., 2005. Unified segmentation. Neuroimage 26, 839–851. doi:10.1016/j.neuroimage.2005.02.018.

Backonja, U., Hall, A.K., Painter, I., Kneale, L., Lazar, A., Cakmak, M., Thompson, H.J., Demiris, G., 2018. Comfort and attitudes towards robots among young, middle-aged, and older adults: a cross-sectional study. J. Nurs. Scholarsh. 50 (6), 623–633. doi:10.1111/jnu.12430.

Baltes, P.B., Lindenberger, U., 1997. Emergence of a powerful connection between sensory and cognitive functions across the adult life span: a new window to the study of cognitive aging? Psychol. Aging 12 (1), 12. doi:10.1037/0882-7974.12.1.12.

Bassett, D.S., Wymbs, N.F., Porter, M.A., Mucha, P.J., Carlson, J.M., Grafton, S.T., 2011. Dynamic reconfiguration of human brain networks during learning. Proc. Natl. Acad. Sci. U. S. A. 108 (18), 7641–7646. doi:10.1073/pnas.1018985108.

Benton, A.L., Abigail, B., Sivan, A.B., Hamsher, K.d., Varney, N.R., Spreen, O., 1994. Contributions to Neuropsychological assessment: A clinical Manual. Oxford University Press, USA.

Bethlehem, R.A., Paquola, C., Seidlitz, J., Ronan, L., Bernhardt, B., Tsvetanov, K.A., Consortium, C.C., 2020. Dispersion of functional gradients across the adult lifespan. Neuroimage 222, 117299. doi:10.1016/j.neuroimage.2020.117299.

Betzel, R.F., Byrge, L., He, Y., Goñi, J., Zuo, X.N., Sporns, O., 2014. Changes in structural and functional connectivity among resting-state networks across the human lifespan. Neuroimage 102, 345–357. doi:10.1016/j.neuroimage.2014.07.067.

Bookheimer, S.Y., Salat, D.H., Terpstra, M., Ances, B.M., Barch, D.M., Buckner, R.L., Burgess, G.C., Curtiss, S.W., Diaz-Santos, M., Elam, J.S., 2019. The lifespan human connectome project in aging: an overview. Neuroimage 185, 335–348. doi:10.1016/j.neuroimage.2018.10.009.

Bordier, C., Nicolini, C., Forcellini, G., Bifone, A., 2018. Disrupted modular organization of primary sensory brain areas in schizophrenia. NeuroImage: Clinical 18, 682–693. doi:10.1016/j.nicl.2018.02.035.

Bullmore, E., Sporns, O., 2009. Complex Brain Networks: graph theoretical Analysis of Structural and Functional Systems. Nat. Rev., Neurosci. 10 (3), 186–198. doi:10.1038/nrn2575.

Calhoun, V.D., Kiehl, K.A., Pearlson, G.D., 2008. Modulation of temporally coherent brain networks estimated using ICA at rest and during cognitive tasks. Hum. Brain Mapp. 29 (7), 828–838. doi:10.1002/hbm.20581.

Campbell, K.L., Samu, D., Davis, S.W., Geerligs, L., Mustafa, A., Tyler, L.K., 2016. Robust resilience of the frontotemporal syntax system to aging. J. Neurosci. 36 (19), 5214–5227. doi:10.1523/JNEUROSCI.4561-15.2016.

Cao, M., Wang, J.H., Dai, Z.J., Cao, X.Y., Jiang, L.L., Fan, F.M., Song, X.W., Xia, M.R., Shu, N., Dong, Q., 2014. Topological organization of the human brain functional connectome across the lifespan. Dev. Cogn. Neurosci. 7, 76–93. doi:10.1016/j.dcn.2013.11.004.

Carpenter, P.A., Just, M.A., Shell, P., 1990. What one intelligence test measures: a theoretical account of the processing in the Raven Progressive Matrices Test. Psychol. Rev. 97 (3), 404. doi:10.1037/0033-295X.97.3.404.

Carr, V.A., Bernstein, J.D., Favila, S.E., Rutt, B.K., Kerchner, G.A., Wagner, A.D., 2017. Individual differences in associative memory among older adults explained by hippocampal subfield structure and function. Proc. Natl. Acad. Sci. U. S. A. 114 (45), 12075–12080. doi:10.1073/pnas.1713308114.

Cassady, K., Ruitenberg, M.F., Reuter-Lorenz, P.A., Tommerdahl, M., Seidler, R.D., 2020. Neural dedifferentiation across the lifespan in the motor and somatosensory systems. Cereb. Cortex 30 (6), 3704–3716. doi:10.1093/cercor/bhz336.

Cattell, R.B., 1971. Abilities: Their structure, growth, and Action. Elsevier.

Chan, M.Y., Park, D.C., Savalia, N.K., Petersen, S.E., Wig, G.S., 2014. Decreased segregation of brain systems across the healthy adult lifespan. Proc. Natl. Acad. Sci. U. S. A. 111 (46), E4997–E5006. doi:10.1073/pnas.1415122111.

Chandan, S., Jia, L., Lv, P., Sun, H., Xiao, Y., Liu, J., Zhao, Y., Zhang, W., Yao, L., Gong, Q., 2018. Age related changes in topological properties of brain functional network and structural connectivity. Front. Neuro. 12. doi:10.3389/fnins.2018.00318, 318-.

Chen, X., Necus, J., Peraza, L.R., Mehraram, R., Wang, Y., O'Brien, J.T., Blamire, A., Kaiser, M., Taylor, J.P., 2021. The functional brain favours segregated modular connectivity at old age unless affected by neurodegeneration. Commun. Biol. 4, 1–16. doi:10.1038/s42003-021-02497-0.

Cohen, J.R., D'Esposito, M., 2016. The segregation and integration of distinct brain networks and their relationship to cognition. J. Neurosci. 36 (48), 12083–12094. doi:10.1523/JNEUROSCI.2965-15.2016.

Cole, M.W., Reynolds, J.R., Power, J.D., Repovs, G., Anticevic, A., Braver, T.S., 2013. Multi-task connectivity reveals flexible hubs for adaptive task control. Nat. Neurosci. 16 (9), 1348–1355. doi:10.1038/nn.3470.

Craik, F.I., 1994. Memory changes in normal aging. Curr. Dir. Psychol. Sci. 3 (5), 155–158. doi:10.1111/1467-8721.ep10770653.

Cui, Z., Li, H., Xia, C.H., Larsen, B., Adebimpe, A., Baum, G.L., Cieslak, M., Gur, R.E., Gur, R.C., Moore, T.M., 2020. Individual variation in functional topography of association networks in youth. Neuron 106 (2), 340–353. doi:10.1016/j.neuron.2020.01.029, e348.

Damoiseaux, J.S., 2017. Effects of aging on functional and structural brain connectivity. Neuroimage 160, 32–40. doi:10.1016/j.neuroimage.2017.01.077.

Danon, L., Diaz-Guilera, A., Duch, J., Arenas, A., 2005. Comparing community structure identification. J. Stat. Mech. (09) 2005P09008.

Deb, K., Agrawal, S., Pratap, A., Meyarivan, T., 2002. A Fast Elitist Non-dominated Sorting Genetic Algorithm for Multi-objective Optimization: NSGA-II. In: International Conference on Parallel Problem Solving from Nature, pp. 849–858.

Dosenbach, N.U., Fair, D.A., Cohen, A.L., Schlaggar, B.L., Petersen, S.E., 2008. A dual-networks architecture of top-down control. Trends Cogn. Sci. 12 (3), 99–105. doi:10.1016/j.tics.2008.01.001.

Ellefsen, K.O., Mouret, J.B., Clune, J., 2015. Neural modularity helps organisms evolve to learn new skills without forgetting old skills. Plos Comput. Biology 11 (4), e1004128. doi:10.1371/journal.pcbi.1004128.

Feng, X., Lipton, Z.C., Yang, J., Small, S.A., Provenzano, F.A.Alzheimer's Disease Neuroimaging Initiative, Frontotemporal Lobar Degeneration Neuroimaging Initiative, 2020. Estimating brain age based on a uniform healthy population with deep learning and structural magnetic resonance imaging. Neurobiol. Aging 91, 15–25. doi:10.1016/j.neurobiolaging.2020.02.009.

Ferreira, L.K., Busatto, G.F., 2013. Resting-state functional connectivity in normal brain aging. Neurosci. Biobehav. Rev. 37 (3), 384–400. doi:10.1016/j.neubiorev.2013.01.017.

Fox, M.D., Zhang, D., Snyder, A.Z., Raichle, M.E., 2009. The global signal and observed anticorrelated resting state brain networks. J. Neurophysiol. 101 (6), 3270–3283. doi:10.1152/jn.90777.2008.

Fries, P., 2005. A mechanism for cognitive dynamics: neuronal communication through neuronal coherence. Trends Cogn. Sci. 9 (10), 474–480. doi:10.1016/j.tics.2005.08.011.

Friston, K.J., Williams, S., Howard, R., Frackowiak, R.S., Turner, R., 1996. Movement-related effects in fMRI time-series. Magn. Reson. Med. 35 (3), 346–355. doi:10.1002/mrm.1910350312.

Garzón, B., Lövdén, M., de Boer, L., Axelsson, J., Riklund, K., Bäckman, L., Nyberg, L., Guitart-Masip, M., 2021. Role of dopamine and gray matter density in aging effects and individual differences of functional connectomes. Brain Struct. Funct. 1–16. doi:10.1007/s00429-020-02205-4.

Geerligs, L., Renken, R.J., Saliasi, E., Maurits, N.M., Lorist, M.M., 2015. A Brain-wide Study of Age-related Changes in Functional Connectivity. Cereb. Cortex 25 (7), 1987–1999. doi:10.1093/cercor/bhu012.

Geerligs, L., Rubinov, M., Cam, C., Henson, R.N., 2015. State and trait components of functional connectivity: individual differences vary with mental state. J. Neurosci. 35, 13949–13961. doi:10.1523/JNEUROSCI.1324-15.2015.

Grady, C., 2012. The cognitive neuroscience of ageing. Nat. Rev., Neurosci. 13 (7), 491–505. doi:10.1038/nrn3256.

Grady, C., Sarraf, S., Saverino, C., Campbell, K., 2016. Age differences in the functional interactions among the default, frontoparietal control, and dorsal attention networks. Neurobiol. Aging 41, 159–172. doi:10.1016/j.neurobiolaging.2016.02.020.

Greicius, M.D., Krasnow, B., Reiss, A.L., Menon, V., 2003. Functional connectivity in the resting brain: a network analysis of the default mode hypothesis. Proc. Natl. Acad. Sci. U. S. A. 100 (1), 253–258. doi:10.1073/pnas.0135058100.

Grunewald, M., Kumar, S., Sharife, H., Volinsky, E., Gileles-Hillel, A., Licht, T., Permyakova, A., Hinden, L., Azar, S., Friedmann, Y., 2021. Counteracting age-related VEGF signaling insufficiency promotes healthy aging and extends life span. Science 373 (6554). doi:10.1126/science.abc8479, eabc8479.

Guo, C.C., Kurth, F., Zhou, J., Mayer, E.A., Eickhoff, S.B., Kramer, J.H., Seeley, W.W., 2012. One-year test–retest reliability of intrinsic connectivity network fMRI in older adults. Neuroimage 61 (4), 1471–1483. doi:10.1016/j.neuroimage.2012.03.027.

Gusnard, D.A., Akbudak, E., Shulman, G.L., Raichle, M.E., 2001. Medial prefrontal cortex

and self-referential mental activity: relation to a default mode of brain function. Proc. Natl. Acad. Sci. U. S. A. 98 (7), 4259–4264. doi:10.1073/pnas.071043098.
Hayes, A.F., 2017. Introduction to mediation, moderation, and Conditional Process analysis: A regression-Based Approach. Guilford publications.
Huntenburg, J.M., Bazin, P.L., Margulies, D.S., 2018. Large-scale gradients in human cortical organization. Trend. Cogn. Sci. 22 (1), 21–31. doi:10.1016/j.tics.2017.11.002.
Hwang, K., Bertolero, M.A., Liu, W.B., D'esposito, M., 2017. The human thalamus is an integrative hub for functional brain networks. J. Neurosci. 37 (23), 5594–5607. doi:10.1523/JNEUROSCI.0067-17.2017.
Jager, G., Kahn, R.S., Van Den Brink, W., Van Ree, J.M., Ramsey, N.F., 2006. Long-term effects of frequent cannabis use on working memory and attention: an fMRI study. Psychopharmacology (Berl.) 185 (3), 358–368. doi:10.1007/s00213-005-0298-7.
Jenkinson, M., Bannister, P., Brady, M., Smith, S., 2002. Improved optimization for the robust and accurate linear registration and motion correction of brain images. Neuroimage 17 (2), 825–841. doi:10.1006/nimg.2002.1132.
Jones, D.T., Vemuri, P., Murphy, M.C., Gunter, J.L., Senjem, M.L., Machulda, M.M., Przybelski, S.A., Gregg, B.E., Kantarci, K., Knopman, D.S., 2012. Non-stationarity in the "resting brain's" modular architecture. PLoS ONE 7 (6), e39731. doi:10.1371/journal.pone.0039731.
Kievit, R.A., Davis, S.W., Mitchell, D.J., Taylor, J.R., Duncan, J., Henson, R.N., 2014. Distinct aspects of frontal lobe structure mediate age-related differences in fluid intelligence and multitasking. Nat. Commun. 5 (1), 1–10. doi:10.1038/ncomms6658.
Kong, R., Li, J., Orban, C., Sabuncu, M.R., Liu, H., Schaefer, A., Sun, N., Zuo, X.-.N., Holmes, A.J., Eickhoff, S.B., 2019. Spatial topography of individual-specific cortical networks predicts human cognition, personality, and emotion. Cereb. Cortex 29 (6), 2533–2551. doi:10.1093/cercor/bhy123.
Lancichinetti, A., Fortunato, S., Kertész, J., 2008. Detecting the overlapping and hierarchical community structure in complex networks. N. J. Phys. 11 (3), 19–44. doi:10.1088/1367-2630/11/3/033015.
Lázár, A., Ábel, D., Vicsek, T., 2009. Modularity Measure of Networks With Overlapping Modules. EPL 90, 983 2010.
Li, S., Lindenberger, U., Sikström, S., 2001. Aging cognition: from neuromodulation to representation. Trend. Cogn. Sci. 5 (11), 479–486. doi:10.1016/S1364-6613(00)01769-1.
Li, Y., Wang, X., Li, Y., Sun, Y., Sheng, C., Li, H., Li, X., Yu, Y., Chen, G., Hu, X., 2016. Abnormal resting-state functional connectivity strength in mild cognitive impairment and its conversion to Alzheimer's disease. Neural Plast doi:10.1155/2016/4680972, 2016.
Liang, X., Zou, Q., He, Y., Yang, Y., 2013. Coupling of functional connectivity and regional cerebral blood flow reveals a physiological basis for network hubs of the human brain. Proc. Natl. Acad. Sci. U. S. A. 110, 1929–1934. doi:10.1073/pnas.1214900110.
Liao, X., Cao, M., Xia, M., He, Y., 2017. Individual differences and time-varying features of modular brain architecture. Neuroimage 152, 94–107. doi:10.1016/j.neuroimage.2017.02.066.
Lin, Y., Ma, J., Gu, Y., Yang, S., Li, L.M.W., Dai, Z., 2018. Intrinsic overlapping modular organization of human brain functional networks revealed by a multiobjective evolutionary algorithm. Neuroimage 181, 430–445. doi:10.1016/j.neuroimage.2018.07.019.
Ma, L., Tian, L., Hu, T., Jiang, T., Zuo, N., 2021. Development of individual variability in brain functional connectivity and capability across the adult lifespan. Cereb. Cortex. 31, 3925–3938. doi:10.1093/cercor/bhab059.
Malagurski, B., Liem, F., Oschwald, J., Mérillat, S., Jäncke, L., 2020. Functional dedifferentiation of associative resting state networks in older adults–A longitudinal study. Neuroimage 214, 116680. doi:10.1016/j.neuroimage.2020.116680.
Margulies, D.S., Ghosh, S.S., Goulas, A., Falkiewicz, M., Huntenburg, J.M., Langs, G., Bezgin, G., Eickhoff, S.B., Castellanos, F.X., Petrides, M., 2016. Situating the default-mode network along a principal gradient of macroscale cortical organization. Proc. Natl. Acad. Sci. U. S. A. 113 (44), 12574–12579. doi:10.1073/pnas.1608282113.
Meunier, D., Achard, S., Morcom, A., Bullmore, E., 2009a. Age-related changes in modular organization of human brain functional networks. Neuroimage 44 (3), 715–723. doi:10.1016/j.neuroimage.2008.09.062.
Meunier, D., Lambiotte, R., Fornito, A., Ersche, K., Bullmore, E.T., 2009b. Hierarchical modularity in human brain functional networks. Front. Neuroinf. 3. doi:10.3389/neuro.11.037.2009, 37.
Meunier, D., Lambiotte, R., Bullmore, E.T., 2010. Modular and hierarchically modular organization of brain networks. Front. Neurosci. 4, 200. doi:10.3389/fnins.2010.00200.
Miettinen, K., 2012. Nonlinear multiobjective optimization. Springer Science & Business Media.
Moraschi, M., Mascali, D., Tommasin, S., Gili, T., Hassan, I.E., Fratini, M., DiNuzzo, M., Wise, R.G., Mangia, S., Macaluso, E., Giove, F., 2020. Brain network modularity during a sustained working-memory task. Front. Physiol. 11, 422. doi:10.3389/fphys.2020.00422.
Murphy, K., Birn, R.M., Handwerker, D.A., Jones, T.B., Bandettini, P.A., 2009. The impact of global signal regression on resting state correlations: are anti-correlated networks introduced? Neuroimage 44 (3), 893–905. doi:10.1016/j.neuroimage.2008.09.036.
Murphy, K., Fox, M.D., 2017. Towards a consensus regarding global signal regression for resting state functional connectivity MRI. Neuroimage 154, 169–173. doi:10.1016/j.neuroimage.2016.11.052.
Najafi, M., Mcmenamin, B.W., Simon, J.Z., Pessoa, L., 2016. Overlapping communities reveal rich structure in large-scale brain networks during rest and task conditions. Neuroimage 135. doi:10.1016/j.neuroimage.2016.04.054.
Newman, M.E., 2004. Fast algorithm for detecting community structure in networks. Phy. Rev. E 69 (6), 066133. doi:10.1103/PhysRevE.69.066133.
Nyberg, L., Salami, A., Andersson, M., Eriksson, J., Kalpouzos, G., Kauppi, K., Lind, J., Pudas, S., Persson, J., Nilsson, .L..-G., 2010. Longitudinal evidence for diminished frontal cortex function in aging. Proc. Natl. Acad. Sci. U. S. A. 107 (52), 22682–22686. doi:10.1073/pnas.1012651108.
Park, D.C., Polk, T.A., Park, R., Minear, M., Savage, A., Smith, M.R., 2004. Aging reduces neural specialization in ventral visual cortex. Proc. Natl. Acad. Sci. U. S. A. 101 (35), 13091–13095. doi:10.1073/pnas.0405148101.
Power, J.D., Cohen, A.L., Nelson, S.M., Wig, G.S., Petersen, S.E., 2011. Functional network organization of the human brain. Neuron 72 (4), 665–678. doi:10.1016/j.neuron.2011.09.006.
Power, J.D., Schlaggar, B.L., Lessov-Schlaggar, C.N., Petersen, S.E., 2013. Evidence for hubs in human functional brain networks. Neuron 79 (4), 798–813. doi:10.1016/j.neuron.2013.07.035.
Preacher, K.J., Hayes, A.F., 2004. SPSS and SAS procedures for estimating indirect effects in simple mediation models. Behav. Res. Meth. Instrum. Comput. 36 (4), 717–731. doi:10.3758/BF03206553.
Preacher, K.J., Hayes, A.F., 2008. Asymptotic and resampling strategies for assessing and comparing indirect effects in multiple mediator models. Behav. Res. Methods 40 (3), 879–891. doi:10.3758/BRM.40.3.879.
Puxeddu, M.G., Faskowitz, J., Betzel, R.F., Petti, M., Astolfi, L., Sporns, O., 2020. The modular organization of brain cortical connectivity across the human lifespan. Neuroimage 218, 116974. doi:10.1016/j.neuroimage.2020.116974.
Raichle, M.E., MacLeod, A.M., Snyder, A.Z., Powers, W.J., Gusnard, D.A., Shulman, G.L., 2001. A default mode of brain function. Proc. Natl. Acad. Sci. U. S. A. 98 (2), 676–682. doi:10.1073/pnas.98.2.676.
Raz, N., Gunning, F.M., Head, D., Dupuis, J.H., McQuain, J., Briggs, S.D., Loken, W.J., Thornton, A.E., Acker, J.D., 1997. Selective aging of the human cerebral cortex observed in vivo: differential vulnerability of the prefrontal gray matter. Cereb. Cortex 7 (3), 268–282. doi:10.1093/cercor/7.3.268.
Rieck, J.R., Baracchini, G., Nichol, D., Abdi, H., Grady, C.L., 2021. Reconfiguration and dedifferentiation of functional networks during cognitive control across the adult lifespan. Neurobiol. Aging 106, 80–94. doi:10.1016/j.neurobiolaging.2021.03.019.
Rubinov, M., Sporns, O., 2010. Complex network measures of brain connectivity: uses and interpretations. Neuroimage 52 (3), 1059–1069. doi:10.1016/j.neuroimage.2009.10.003.
Sadaghiani, S., Kleinschmidt, A., 2013. Functional interactions between intrinsic brain activity and behavior. Neuroimage 80, 379–386. doi:10.1016/j.neuroimage.2013.04.100.
Sala-Llonch, R., Junque, C., Arenaza-Urquijo, E.M., Vidal-Pineiro, D., Valls-Pedret, C., Palacios, E.M., Domenech, S., Salva, A., Bargallo, N., Bartres-Faz, D., 2014. Changes in whole-brain functional networks and memory performance in aging. Neurobiol. Aging 35 (10), 2193–2202. doi:10.1016/j.neurobiolaging.2014.04.007.
Salami, A., Wåhlin, A., Kaboodvand, N., Lundquist, A., Nyberg, L., 2016. Longitudinal evidence for dissociation of anterior and posterior MTL resting-state connectivity in aging: links to perfusion and memory. Cereb. Cortex 26 (10), 3953–3963. doi:10.1093/cercor/bhw233.
Samu, D., Campbell, K.L., Tsvetanov, K.A., Shafto, M.A., Tyler, L.K., 2017. Preserved cognitive functions with age are determined by domain-dependent shifts in network responsivity. Nat. Commun. 8 (1), 1–14. doi:10.1038/ncomms14743.
Staffaroni, A.M., Cobigo, Y., Elahi, F.M., Casaletto, K.B., Walters, S.M., Wolf, A., Lindbergh, C.A., Rosen, H.J., Kramer, J.H., 2019. A longitudinal characterization of perfusion in the aging brain and associations with cognition and neural structure. Hum. Brain Mapp. 40 (12), 3522–3533. doi:10.1002/hbm.24613.
Schwarz, G., 1978. Estimating the dimension of a model. Ann. Stat. 6 (2), 461–464. http://www.jstor.org/stable/2958889.
Shafto, M.A., Tyler, L.K., Dixon, M., Taylor, J.R., Rowe, J.B., Cusack, R., Calder, A.J., Marslen-Wilson, W.D., Duncan, J., Dalgleish, T., 2014. The Cambridge Centre for Ageing and Neuroscience (Cam-CAN) study protocol: a cross-sectional, lifespan, multidisciplinary examination of healthy cognitive ageing. BMC Neurol 14 (1), 1–25. doi:10.1186/s12883-014-0204-1.
Song, J., Birn, R.M., Boly, M., Meier, T.B., Nair, V.A., Meyerand, M.E., Prabhakaran, V., 2014. Age-related reorganizational changes in modularity and functional connectivity of human brain networks. Brain Connect 4, 662–676. doi:10.1089/brain.2014.0286.
Sporns, O., Betzel, R.F., 2016. Modular brain networks. Annu. Rev. Psychol. 67, 613–640. doi:10.1146/annurev-psych-122414-033634.
Spreng, R.N., Stevens, W.D., Viviano, J.D., Schacter, D.L., 2016. Attenuated anticorrelation between the default and dorsal attention networks with aging: evidence from task and rest. Neurobiol. Aging 45, 149–160. doi:10.1016/j.neurobiolaging.2016.05.020.
Telesford, Q.K., Simpson, S.L., Burdette, J.H., Hayasaka, S., Laurienti, P.J., 2011. The brain as a complex system: using network science as a tool for understanding the brain. Brain Connet 1 (4), 295–308. doi:10.1089/brain.2011.0055.
Van Den Heuvel, M.P., Pol, H.E.H., 2010. Exploring the brain network: a review on resting-state fMRI functional connectivity. Eur. Neuropsychopharmacol. 20 (8), 519–534. doi:10.1016/j.euroneuro.2010.03.008.
Wang, D., Buckner, R.L., Fox, M.D., Holt, D.J., Holmes, A.J., Stoecklein, S., Langs, G., Pan, R., Qian, T., Li, K., 2015. Parcellating cortical functional networks in individuals. Nat. Neurosci. 18 (12), 1853–1860. doi:10.1038/nn.4164.
Wang, J., Wang, X., Xia, M., Liao, X., Evans, A., He, Y., 2015. GRETNA: a graph theoretical network analysis toolbox for imaging connectomics. Front. Hum. Neurosci. 9. doi:10.3389/fnhum.2015.00386.
Wen, X., Chen, W., Lin, Y., Gu, T., Zhang, H., Li, Y., Yin, Y., Zhang, J., 2016. A maximal clique based multiobjective evolutionary algorithm for overlapping community detection. IEEE Trans. Evol. Comput. 21 (3), 363–377. doi:10.1109/TEVC.2016.2605501.
Wen, X., Zhang, H., Li, G., Liu, M., Yin, W., Lin, W., Zhang, J., Shen, D., 2019. First-year development of modules and hubs in infant brain functional networks. Neuroimage 185, 222–235. doi:10.1016/j.neuroimage.2018.10.019.
Wink, A.M., 2019. Eigenvector centrality dynamics from resting-state fMRI:

gender and age differences in healthy subjects. Front. Neurosci. 13, 648. doi:10.3389/fnins.2019.00648.
Yan, C., Zang, Y., 2010. DPARSF: a MATLAB toolbox for "pipeline" data analysis of resting-state fMRI. Front., syst. Neurosci. 4. doi:10.3389/fnsys.2010.00013.
Yan, C., Craddock, R.C., He, Y., Milham, M.P., 2013. Addressing head motion dependencies for small-world topologies in functional connectomics. Front. Hum. Neurosci. 7, 910. doi:10.3389/fnhum.2013.00910.
Yang, G.J., Murray, J.D., Repovs, G., Cole, M.W., Savic, A., Glasser, M.F., Pittenger, C., Krystal, J.H., Wang, X.-J., Pearlson, G.D., 2014. Altered global brain signal in schizophrenia. Proc. Natl. Acad. Sci. U. S. A. 111 (20), 7438–7443. doi:10.1073/pnas.1405289111.
Yeo, B.T.T., Krienen, F.M., Sepulcre, J., Sabuncu, M.R., Lashkari, D., Hollinshead, M., Roffman, J.L., Smoller, J.W., Zollei, L., Polimeni, J.R., Fischl, B., Liu, H., Buckner, R.L., 2011. The organization of the human cerebral cortex estimated by intrinsic functional connectivity. J. Neurophysiol. 106, 1125–1165. doi:10.1152/jn.00338.2011.
Yeo, B.T.T., Krienen, F.M., Chee, M.W., Buckner, R.L., 2014. Estimates of segregation and overlap of functional connectivity networks in the human cerebral cortex. Neuroimage 88, 212–227. doi:10.1016/j.neuroimage.2013.10.046.
Yeo, B.T.T., Krienen, F.M., Eickhoff, S.B., Yaakub, S.N., Fox, P.T., Buckner, R.L., Asplund, C.L., Chee, M.W.L., 2015. Functional specialization and flexibility in human association cortex. Cereb. Cortex 25 (10), 3654–3672. doi:10.1093/cercor/bhv260.
Ystad, M., Eichele, T., Lundervold, A.J., Lundervold, A., 2010. Subcortical functional connectivity and verbal episodic memory in healthy elderly—A resting state fMRI study. Neuroimage 52 (1), 379–388. doi:10.1016/j.neuroimage.2010.03.062.
Zimmermann, J., Ritter, P., Shen, K., Rothmeier, S., Schirner, M., McIntosh, A.R., 2016. Structural architecture supports functional organization in the human aging brain at a regionwise and network level. Hum. Brain Mapp. 37, 2645–2661. doi:10.1002/hbm.23200.
Zuo, X.N., He, Y., Betzel, R.F., Colcombe, S., Sporns, O., Milham, M.P., 2017. Human connectomics across the life span. Trends Cogn. Sci. 21 (1), 32–45. doi:10.1016/j.tics.2016.10.005.
Zhang, Y., Wang, Y., Chen, N., Guo, M., Wang, X., Chen, G., Li, Y., Yang, L., Li, S., Yao, Z., Hu, B., 2021. Age-associated differences of modules and hubs in brain functional networks. Front. Aging Neurosci. 12. doi:10.3389/fnagi.2020.607445.
Zhang, J., Zhou, Z., Li, L., Ye, J., Shang, D., Zhong, S., Yao, B., Xu, C., Yu, Y., He, F., Ye, X., Luo, B., 2022. Cerebral perfusion mediated by thalamo-cortical functional connectivity in non-dominant thalamus affects naming ability in aphasia. Hum. Brain Mapp. 43, 940–954. doi:10.1002/hbm.25696.